Kinetic and Thermodynamic Studies of an Epoxy System Diglycidyl Ether of Bisphenol A/1, 2 Diamine Cyclohexane/Calcium Carbonate Filler

LISARDO NÚÑEZ, F. FRAGA, A. CASTRO, M. R. NÚÑEZ, M. VILLANUEVA

Research Group TERBIPROMAT, Departamento de Física Aplicada, Universidad de Santiago, 15706, Santiago, Spain

Received 15 March 1999; accepted 11 June 1999

ABSTRACT: The curing reaction of an epoxy system consisting of a diglycidyl ether of bisphenol A (BADGE $n = 0$) and 1,2-diaminecyclohexane (DCH) with a calcium carbonate filler was studied by differential scanning calorimetry (DSC) and using a scanning electronic microscope (SEM). As a first stage, the optimum content of the filler determined was 20%. From a kinetic study, in which two models were used, parameters such as reaction orders, rate constants, and activation energies were determined. A thermodynamic study allowed calculation of enthalpy ($\Delta H^{\#}$), entropy ($\Delta S^{\#}$), and free-energy (($\Delta G^{\#}$) changes. The results were compared to those obtained for the same epoxy systems without the filler. © 2000 John Wiley & Sons, Inc. J Appl Polym Sci 75: 291–305, 2000

Key words: filled epoxy–amine reactions; DSC; kinetic parameters; thermodynamic study; BADGE ($n = 0$)

INTRODUCTION

The chemistry involved in the epoxy curing process is rather complex and, despite the extensive research that has been done over the years, it is still not completely understood. As a result, it is impossible to describe it rigorously, and existing models always involve certain assumptions and approximations.

The progress of the curing reaction is described quantitatively in terms of the degree of conversion of epoxide groups, usually designated α. To model the kinetics it is necessary to derive an equation expressing the reaction rate, $d\alpha/dt$, as a function of α and the temperature T. The reaction rate of an epoxy system can be expressed by the sum of two mechanisms—nth order and autocatalyzed.

For this study, two kinetic models were used to check the best fit to experimental data. One of them is the kinetic model proposed by Horie et al.,[1] assuming equal reactivity for all amine hydrogens. A general form of reaction rate for this model is

$$\frac{d\alpha}{dt} = (k_1 + k_2\alpha)(1 - \alpha)^n \tag{1}$$

The other one is the kinetic model proposed by Kamal,[2] which developed the following semiempirical equation:

$$\frac{d\alpha}{dt} = (k_1 + k_2\alpha^m)(1 - \alpha)^n \tag{2}$$

The introduction of the variable exponents m and n usually makes it possible to obtain a good fit to experimental data.

Correspondence to: L. Núñez.

Journal of Applied Polymer Science, Vol. 75, 291–305 (2000)
 CCC 0021-8995/00/020291-15

EXPERIMENTAL

Materials

The epoxy resin was a commercial BADGE ($n = 0$) (Resin 332, Sigma Chemical Co., St. Louis, MO) with an equivalent molecular weight of 173.6 g/Eq, as determined by wet analysis.[3,4] The curing agent was 1,2-diaminecyclohexane (DCH) (Fluka, Switzerland), with an amine hydrogen weight of 28.5. The inert filler was calcium carbonate (Analema, Spain).

Sample Preparation

For calorimetric experiments, epoxy resin and filler were carefully and homogeneously mixed before being added the curing agent at a stoichiometric ratio in respect to the epoxy resin. In a different series of experiments, the amount of filler was 10, 15, 20, 25, and 30% of the total weight of the mixture (epoxy/hardener/filler). In every case, bulk samples of 200 mg were prepared. From the bulk samples, 4–7 mg in size samples were used for calorimetric experiments. The samples were sealed, using a press, in aluminium pans before introducing them into the calorimeter.

Differential Scanning Calorimetry (DSC)

A Perkin–Elmer DSC-7 unit, under control of a 1020 system controller was used for calorimetric measurements. Owing to the wide range of temperature (−30–250°C) necessary for this study, the calorimeter was calibrated using two standards (indium and bidistilled water, obtained by the milipore method). For determination of the different kinetic parameters, the calorimeter was operated in isothermal and dynamic modes.

Scanning Electronic Microscope (SEM)

A JEOL Scanning Microscope (JEOL JSM-6400) was used for SEM micrographs. Before being introduced in the SEM, polymeric samples were covered with a 20-μm thickness of a gold coat, under Argon at 0.05 mbar. The coating was made using a BAL-TEC SCD004 Sputter Coater regulated to operate with a 15-μA current. An optimum coating is achieved by placing the sample at 50 mm from the sputter coater for 165 s.

RESULTS AND DISCUSSION

Kinetic Study

As a first stage, this study requires the determination of the optimum filler concentration. With this aim, dynamic experiments using different percentages of filler (10, 15, 20, 25, 30%) were carried out. Three experiments were performed for each concentration. Figure 1 shows enthalpy values corresponding to every experiment. As can be seen, the only reproducible results are those corresponding to 20% filler contents. This may be related to the fact that at lower filler concentrations (10–15%) it is difficult to achieve a good homogenization of the mixture. Because of this, it is impossible to assure that the filler occupies the same positions, and thus the material structure can change. For higher concentrations (25–30%), filler distribution is rather heterogeneous, and acts as a barrier, hindering crosslinking in different zones of the material. Figure 2 shows SEM images corresponding to samples with filler contents in the range of 10–30%. From the economical point of view, our aim is the search for the maximum filler content showing good homogeneity. As can be seen, 20% samples show good homogeneity over the whole surface, while samples with other filler contents present certain heterogeneity that make the reaction mechanism depend on the position of the filler in the network. The position of the calcium carbonate is shown in Figure 2. White zones in the micrographs correspond to the carbonate filler. After determination of the optimum filler contents, which we consider as that with the highest reproducibility in the ΔH vs. filler content plots (20%), dynamic experiments were carried out to measure the enthalpy change for this system. Knowledge of the enthalpy change is necessary for a subsequent isothermal study.

Table I shows ΔH (J/g) values obtained from dynamic experiments performed on the 20% filler content system and for the system without the filler. As can be seen, values for the system with filler are around 40 J/g lower than for the system without.[5] This fact shows that the kinetic mechanism of the system with calcium carbonate filler is less exothermic. From these experiments the T_g for the filled system was also determined, and resulted in being around 128°C. This value, as expected, is lower than the T_g (146°C) reported[5–7] for the nonfilled system.

From the isothermal experiments, a temperature range of 55–110°C was selected based on the fact that temperatures above and just below T_g lead to very low conversions. Enthalpy changes corresponding to the different selected temperatures were determined. Table II shows total enthalpy changes for the system with and without

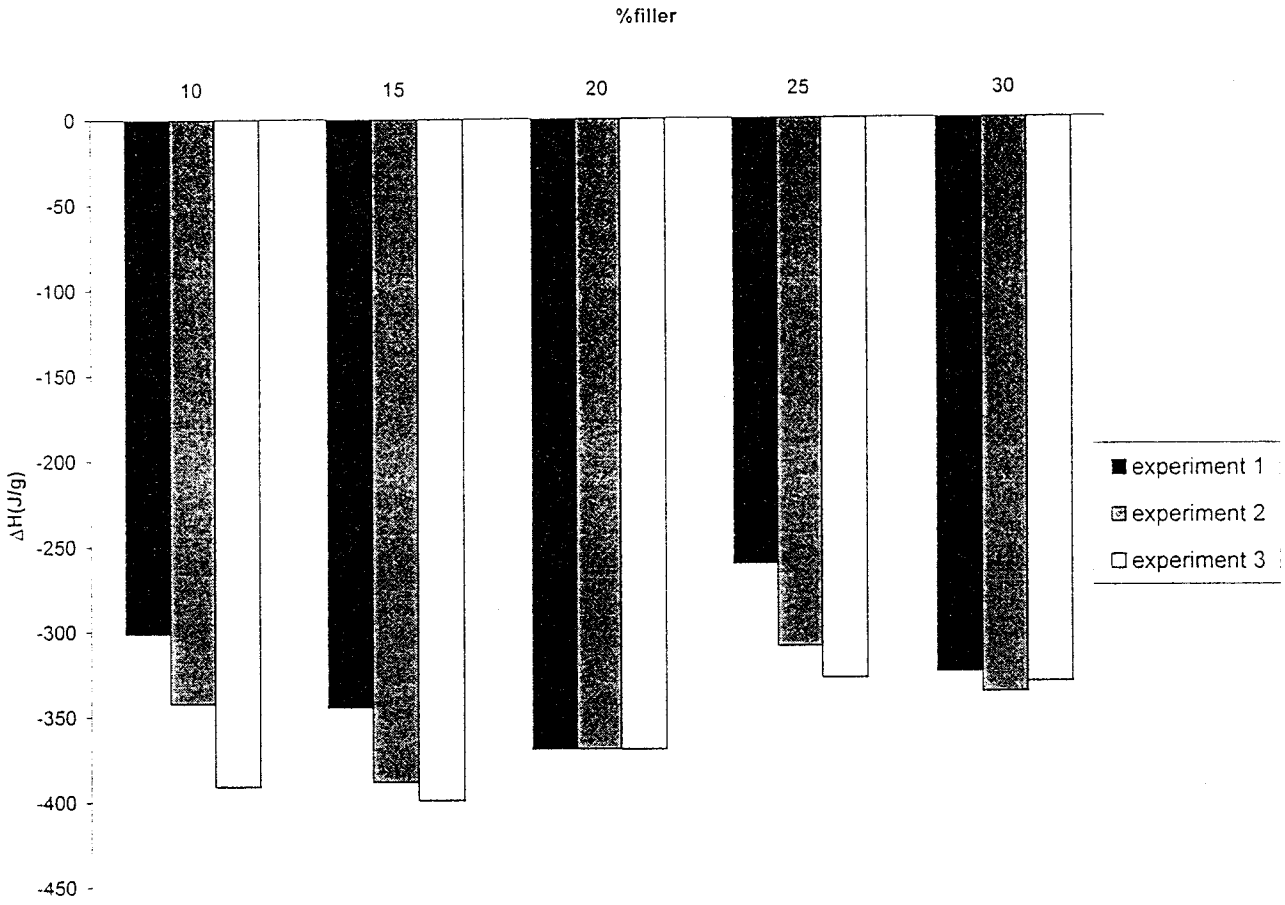

Figure 1 Plots of ΔH versus the filler content (%) for the three experiments carried out on the different samples studied.

filler at the different isothermal temperatures studied. Again, the different isothermal experimental values for the filled system are lower than those obtained for the original epoxy system.

From these values, and the kinetic model used, values of the reaction orders can be determined.

A general expression for degree of conversion, α, is

$$\alpha = \frac{\Delta H_t}{\Delta H_0}$$

where ΔH_t is the heat evolved up to a certain time, in an isothermal experiment, and ΔH_0 the total heat of reaction, obtained from a dynamic experiment.

The reaction rate, $d\alpha/dt$, was determined from DSC experiments using the equation

$$\frac{d\alpha}{dt} = \frac{dH/dt}{\Delta H_0} \quad (3)$$

assuming its proportionality to the rate of heat generation dH/dt.

Figure 3 shows the reaction rates corresponding to the different isothermal temperatures. It can be seen that the reaction rate increases with temperature, but drops faster with increasing temperatures.

Figure 4 shows the degree of conversion as a function of time for the different isothermal temperatures. In this figure, it can be observed that, at every temperature, conversion rapidly increases with curing time reaching a practically constant value. This is due to the fact that an increase in the curing time is followed by an increase in the molecular weight and, because of this, the chains start branching and crosslinking, thus hindering mobility, and consequently crosslinking stops. For the filled system, maximum conversion is 87% at 100°C. Comparison of this value with conversion at the same temperature for the nonfilled system shows a decrease of 10% in conversion. This means that elastic properties of the material are not prac-

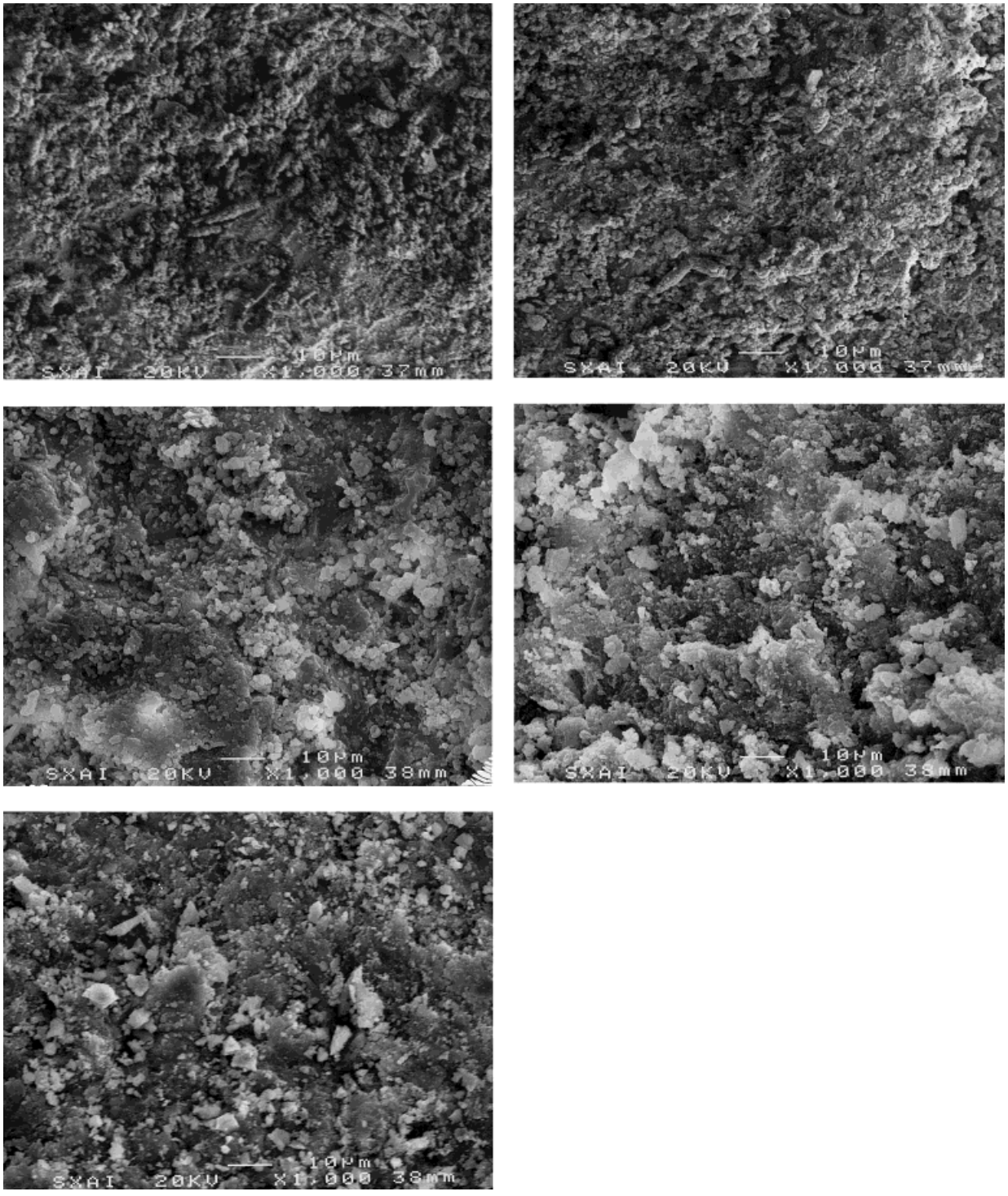

Figure 2 SEM micrographs corresponding to samples with the filler contents in the range of 10–30%.

tically affected, while mechanical properties significantly improved. A future article will report on elastic properties of this material.

The reaction order was determined using the model proposed by Horie et al.,[1] and the reduced rate of reaction, defined as

Table I Values of Enthalpy Changes for the System With and Without Filler

ΔH (J/g)	
Filler	Without Filler
−369.18	−409.8
−369.67	−410.4
−369.72	−414.2
−368.81	—
−367.99	—
Average ≡ −369.07	−411.5
Standard deviation ≡ 0.67	2.72

$$\alpha^0 = \frac{d\alpha/dt}{(1-\alpha)^n} \tag{4}$$

Different values of n were tried to obtain the best linear fitting of the experimental results. Plots of reduced rate, α^0, versus conversion, α, for different n values (0.5, 1, 1.5, and 2) and isothermal temperatures (100, 90, 80, 70, 60, and 55°C) are shown in Figure 5(a–f).

The best linear fitting of the experimental results was achieved for $n = 2$. Once this value was found, it may be concluded that the overall reaction order is 3.

The Kamal[2] kinetic model was used to fit $d\alpha/dt$ versus α plots. Table III shows constant rates, and reaction orders for nth and autocatalytic paths, as well as the overall reaction order, for the different isothermal experiments. Values listed in this table suggest a value of 3 for the overall reaction order, in good agreement with values reported by some other authors[1,5–11] for similar reactions. This result was expected because the filler does not change the reaction mechanism because it only affects crosslinking and, in a previous article,[5] we reported an overall reaction order of 3 for the nonfilled system. Table IV shows rate constants corresponding to the nth order and autocatalytic mechanisms for the filled and non-

Table II Values of Enthalpy Changes from DSC Isothermal Measurements at Different Temperatures for the System With and Without Filler

	ΔH_t (J/g)	
T	Filler	Without Filler
110	−313.23	−389.53
100	−324.17	−400.15
90	−289.94	−391.73
80	−282.96	−378.98
70	−247.27	−334.37
60	−231.81	−282.53
55	−208.92	—

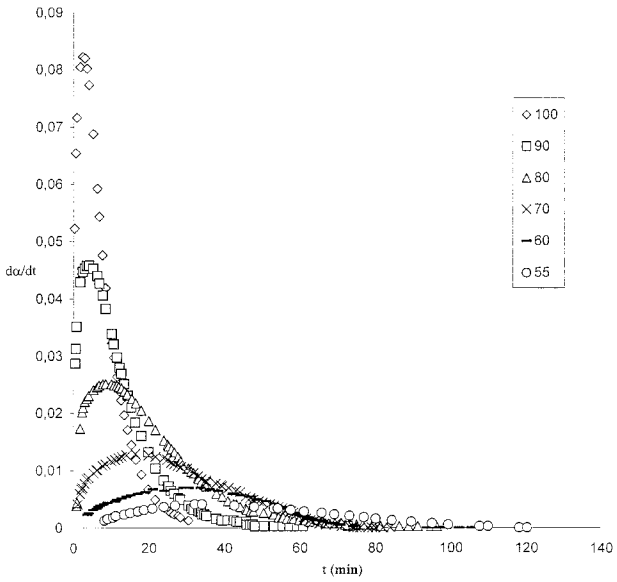

Figure 3 Reaction rate versus time plots for the different isothermal temperatures.

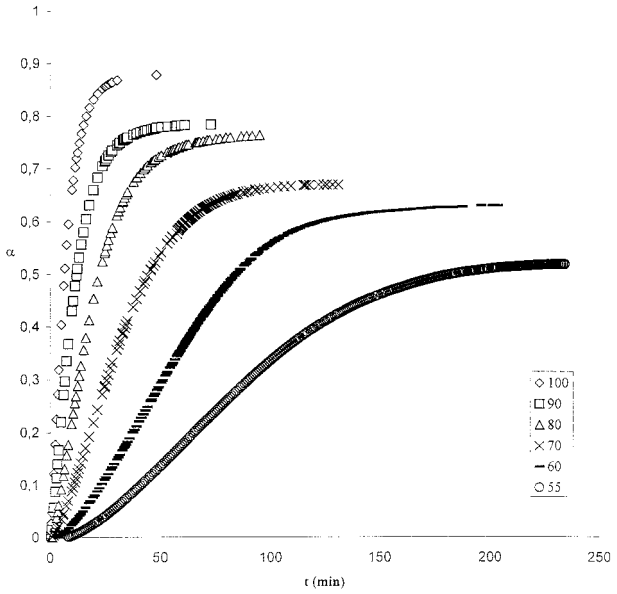

Figure 4 Degree of conversion versus time for the different isothermal temperatures.

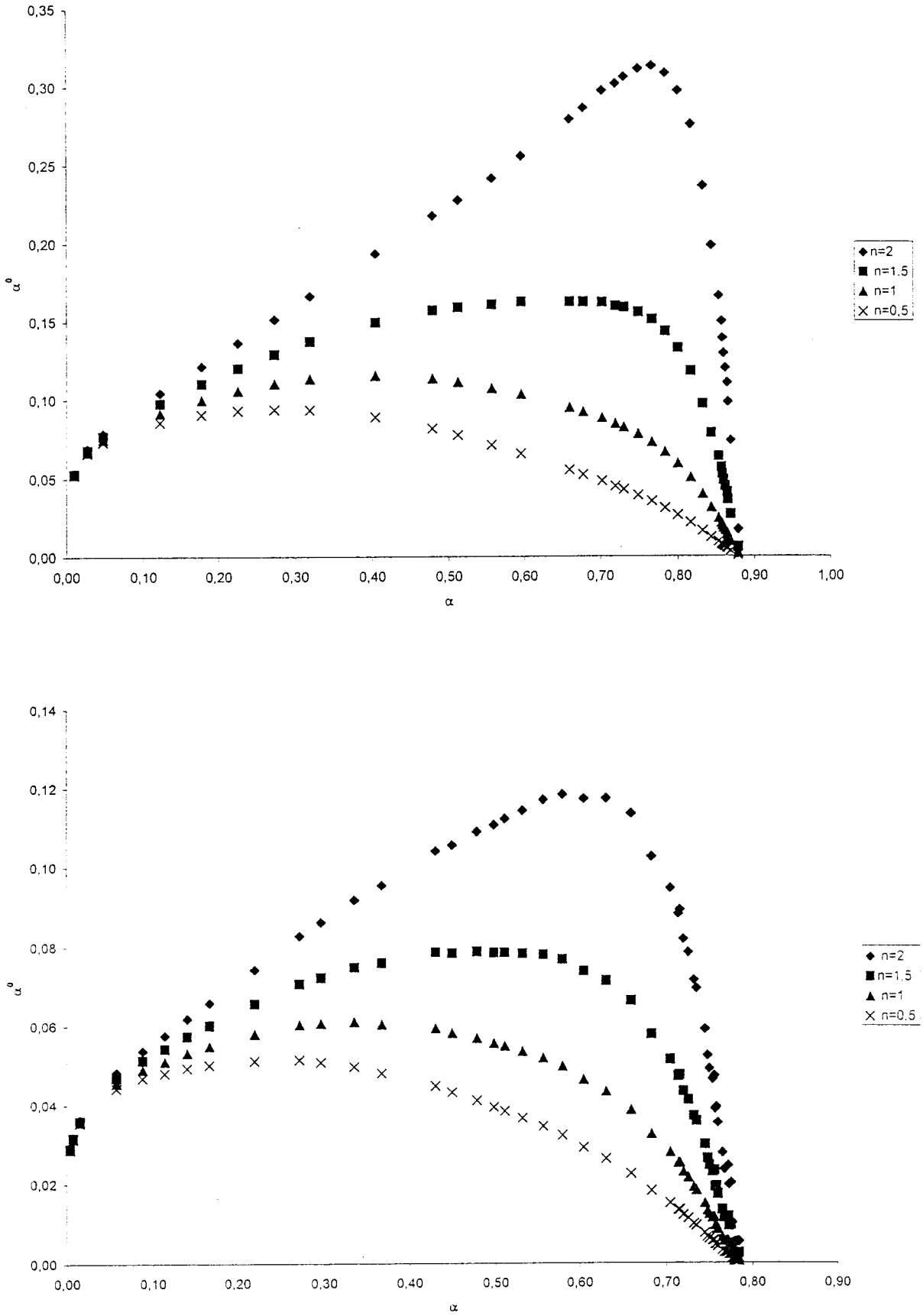

Figure 5 Plots of reduced rate, α^0, versus conversion, α, for different n values (0.5, 1, 1.5, 2) at (a) 100°C, (b) 90°C, (c) 80°C, (d) 70°C, (e) 60°C, and (f) 55°C.

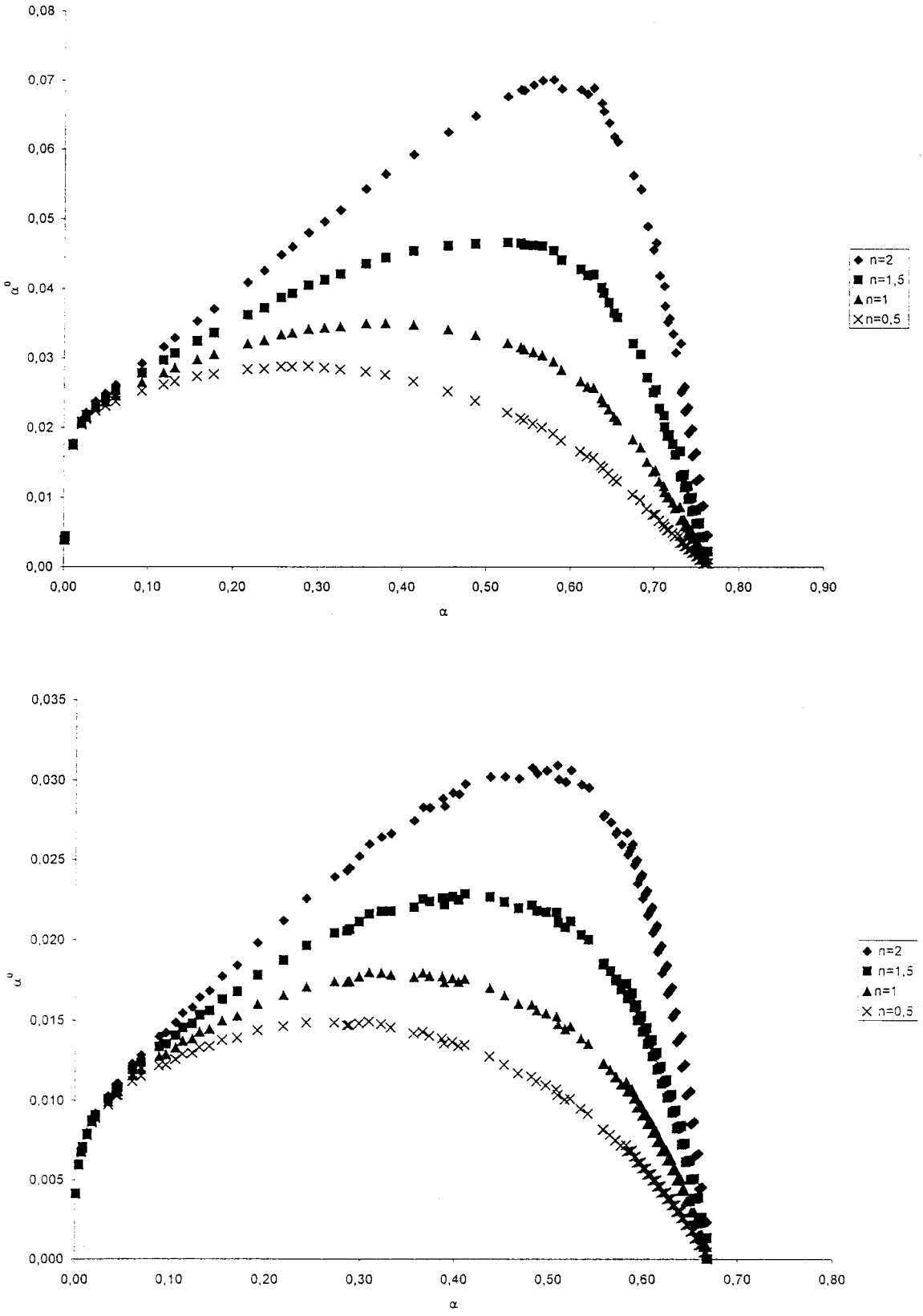

Figure 5 (*Continued from the previous page*)

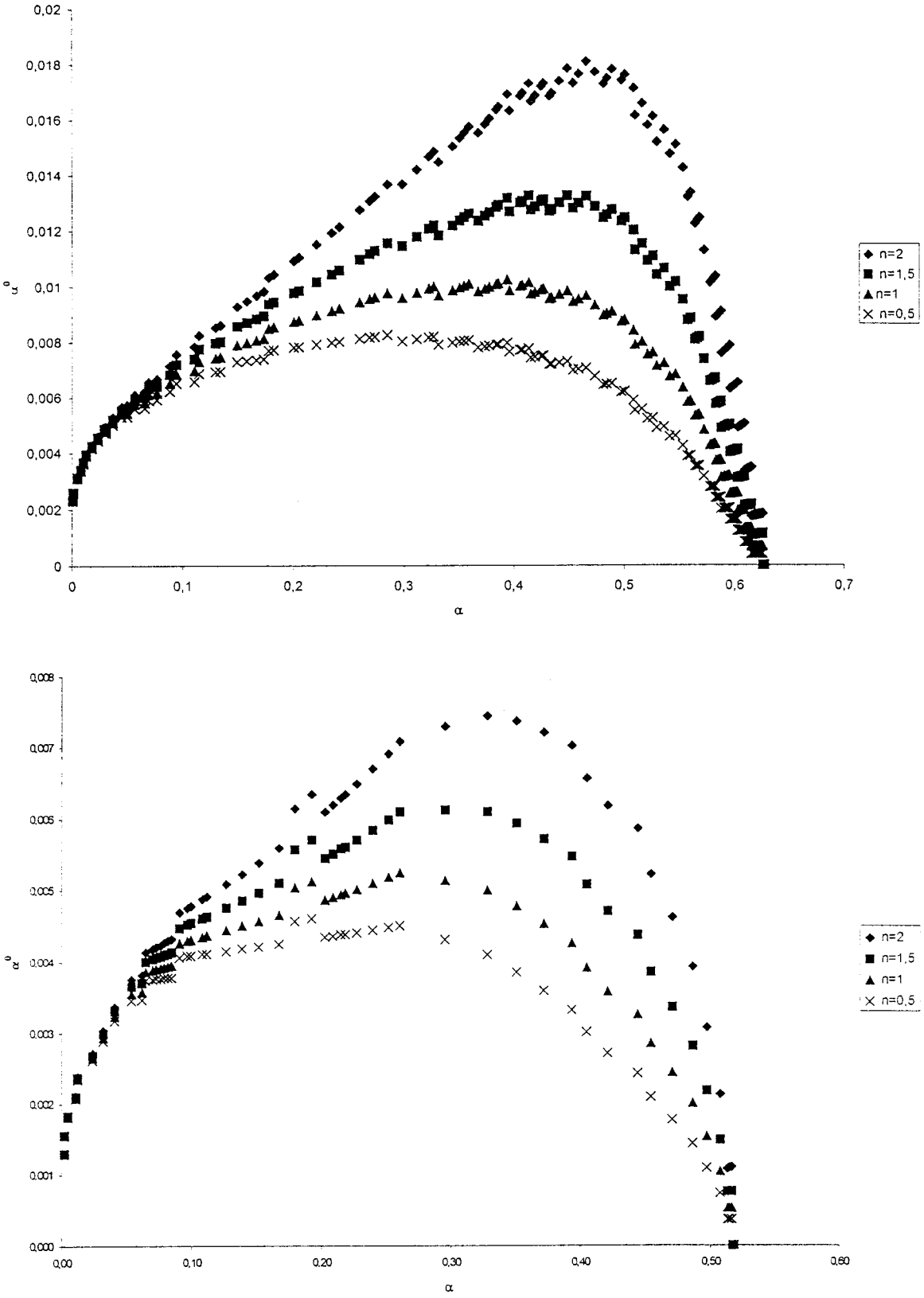

Figure 5 (*Continued from the previous page*)

Table III Values of K_1, K_2, and Reaction Order for the n^{th}, Autocatalyzed Mechanism and Overall Reaction Order for the System With and Without Filler Using the Kamal et al. Model

T	n^{th} Order K_1 (min^{-1})	Autocatalyzed K_2 (min^{-1})	m	n	$m + n$
100	0.070	0.36	1.10	2.07	3.17
90	0.040	0.21	1.08	2.33	3.41
80	0.022	0.14	1.10	2.34	3.44
70	0.0083	0.071	1.00	2.43	3.43
60	0.0042	0.039	1.04	2.24	3.28
55	0.0008	0.014	0.51	2.73	3.24

filled system. This values were calculated using the Horie et al. model. Again, values corresponding to the system with calcium carbonate filler are lower than those for the original system, owing to the filler-hindering effect.

The activation energies corresponding to the two kinetic mechanisms were obtained from the Arrhenius plot of ln k versus 1000/T. Values of these activation energies are shown in Table V. These values are higher for the filled system. This means that the presence of a filler hinders crosslinking between different zones of the material, thus increasing the energy necessary for a three-dimensional network.

To check the best-fitting model, plots of the reaction rate versus time, at the different isothermal temperatures, were made for the experimental data, Horie et al., and Kamal models.

Figure 6 shows that the Kamal model is the one best fitting experimental results at all isothermal-curing temperatures. It may also be observed, for large curing times, at all temperatures, a deviation between the experimental data and kinetic models. This is due to the fact that, from a given conversion, the curing reaction is no longer kinetically controlled, and the curing reaction becomes diffusion controlled. In a future article, a factor accounting for diffusion will be introduced in the kinetic model.

Plots of α versus T, at the different isothermal temperatures, show that the best fitting corresponds to the Kamal model. Also, the best results were found at 100°C, where higher conversion values were achieved. This is in good agreement with the optimum curing temperature, 100°C, found for the nonfilled system.[5]

Table IV Values of K_1 and K_2 for the System With and Without Filler Using Horie et al. Model

	n^{th} Order K_1 (min^{-1})		Autocatalyzed K_2 (min^{-1})	
T	Filler	Without Filler	Filler	Without Filler
100	0.062	0.20	0.33	0.61
90	0.041	0.11	0.15	0.34
80	0.021	0.064	0.093	0.27
70	0.0090	0.039	0.055	0.14
60	0.0042	0.018	0.033	0.09
55	0.0032	—	0.014	—

Thermodynamic Study

Changes of entropy, enthalpy, and Gibbs free energy for thermosets can be evaluated by application of the transition state theory.[12,13] This theory assumes the formation of an activated complex ($ABC^{\#}$) in equilibrium with reactants (A, B, and C) before the formation of the eventual product (P). The scheme is as follows:

$$A + B + C \overset{K^{\#}}{\leftrightarrow} ABC^{\#} \overset{k}{\rightarrow} P$$

Table V Values of Activation Energies Using the Kamal et al. Model for the Two Systems, With and Without Filler

	E_a (kJ/mol)	
	Filler	Without Filler
n^{th} Order	71.81	61.19
Autocatalytic	52.42	47.67

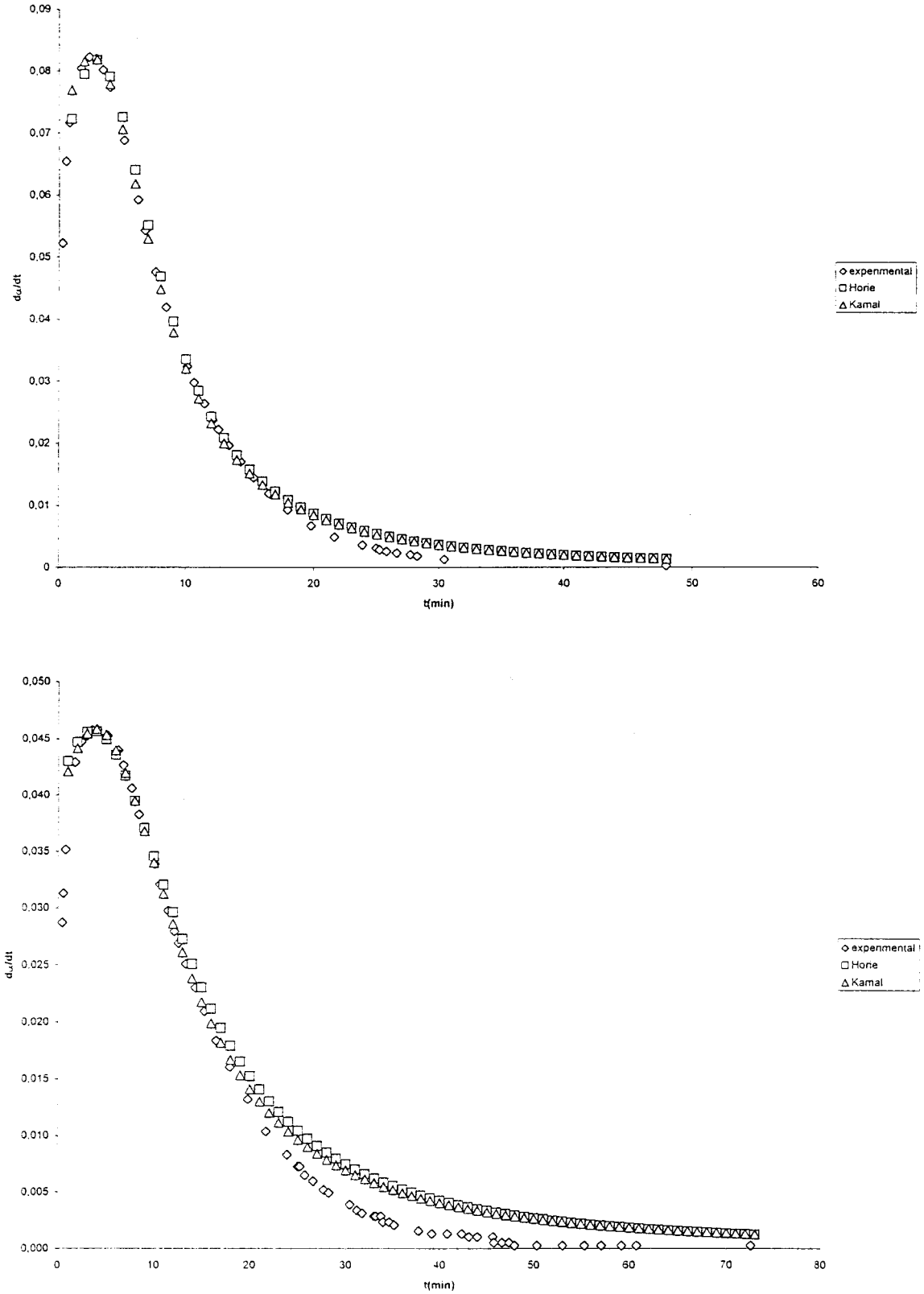

Figure 6 Plots of reaction rate, $d\alpha/dt$, versus time, t. Comparison of experimental data with the Horie and Kamal models at: (a) 100°C, (b) 90°C, (c) 80°C, (d) 70°C, (e) 60°C, and (f) 55°C.

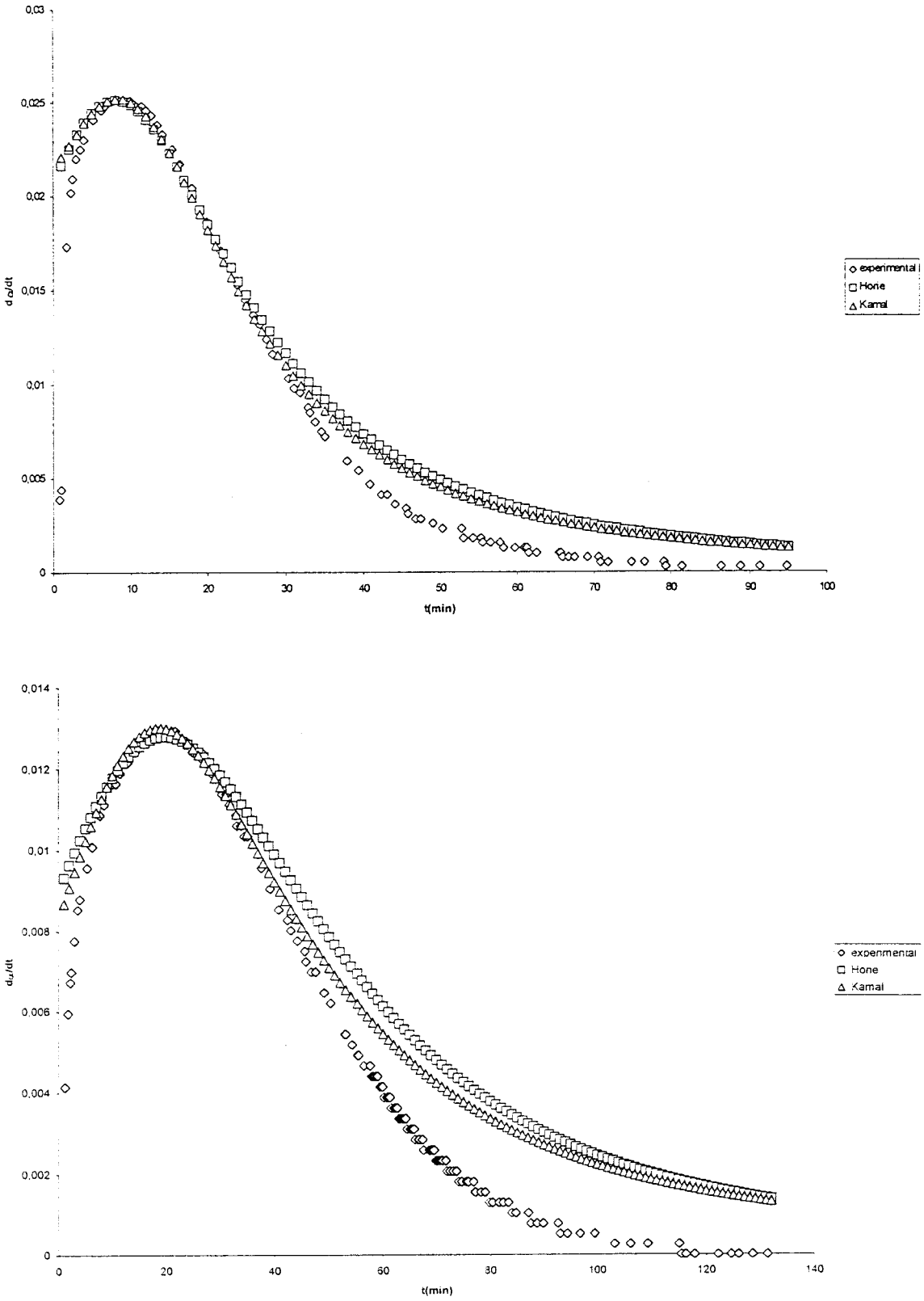

Figure 6 (*Continued from the previous page*)

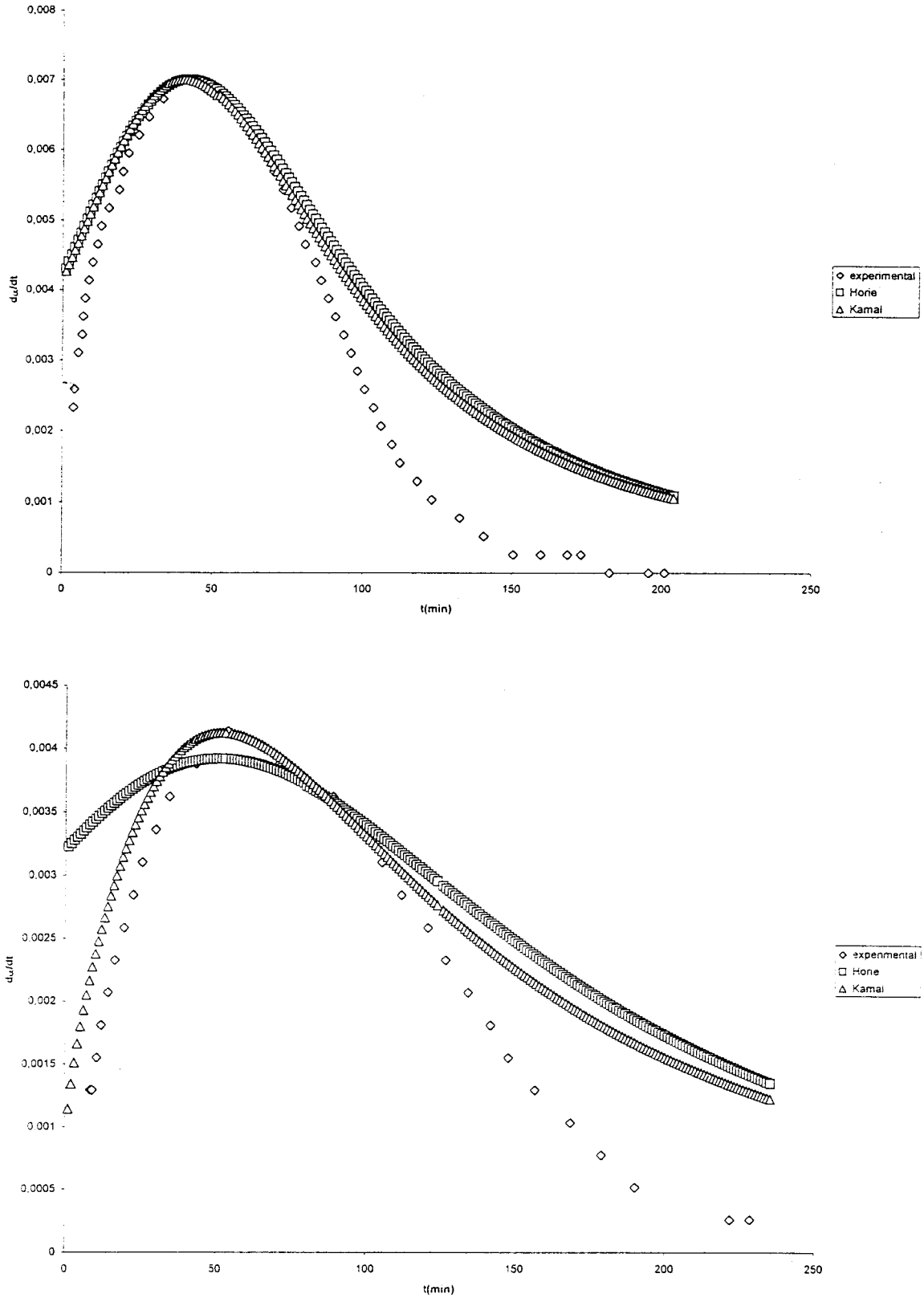

Figure 6 (*Continued from the previous page*)

Table VI Values of Activation Enthalpy and Activation Entropy Changes for the Systems With and Without the Filler

	Filler		Without Filler	
	$\Delta H^{\#}$ (kJ/mol)	$\Delta S^{\#}$ (kJ/mol)	$\Delta H^{\#}$ (kJ/mol)	$\Delta S^{\#}$ (kJ/mol)
n^{th} order path	−71.81	−75.73	−58.3	−104.1
Autocatalyzed path	−54.42	−109.22	−44.7	−131.4

The equilibrium constant $K^{\#}$ for the activation of the transition state can be written as

$$K^{\#} = \frac{[\text{ABC}]^{\#}}{[\text{A}][\text{B}][\text{C}]} \tag{5}$$

where [A], [B], [C], and $[\text{ABC}]^{\#}$ represent concentration of A, B, C, and the activated complex, respectively.

Absolute reaction rate theory has shown that

$$k[\text{A}][\text{B}][\text{C}] = [\text{ABC}]^{\#}\frac{k_B T}{h} \tag{6}$$

where k is the specific reaction rate to form the product, k_B is Boltzmann constant, h is Planck's constant, and T is the absolute temperature.

From the last two equations

$$k = \frac{k_B T}{h} K^{\#} \tag{7}$$

The equilibrium constant $K^{\#}$ is related to the activation free energy change $\Delta G^{\#}$ as follows:

$$\Delta G^{\#} = -RT \ln K^{\#} = \Delta H^{\#} - T\Delta S^{\#}$$

where $\Delta H^{\#}$ is the activation heat of reaction, $\Delta S^{\#}$ the entropy change of activation, and R is the gas constant.

$\Delta G^{\#}$ can also be written as

$$\Delta G^{\#} = -RT \ln \frac{kh}{k_B T} = \Delta H^{\#} - T\Delta S^{\#}$$

Solving for k

$$k = \frac{k_B T}{h} e^{\Delta G^{\#}/RT} \tag{8}$$

or

$$k = \frac{k_B T}{h} e^{\Delta S^{\#}/R}\, e^{-\Delta H^{\#}/RT} \tag{9}$$

This last equation can be written as

$$\frac{k}{T} = \frac{k_B}{h}\, e^{\Delta S^{\#}/R}\, e^{-\Delta H^{\#}/RT}$$

Table VII Gibbs Activation Free Energy Changes Corresponding to the *n*th Order and Autocatalized Mechanisms for the Systems With and Without the Filler

	Filler		Without Filler	
T	$\Delta G_{n\text{th path}}$	ΔG_{auto}	$\Delta G_{n\text{th path ref}}$	ΔG_{auto}
298.15	−49.23	−21.85	−27.24	−5.57
308.15	−48.47	−20.76	−26.20	−4.25
318.15	−47.72	−19.67	−25.16	−2.94
328.15	−46.96	−18.58	−24.12	−1.62
338.15	−46.20	−17.48	−23.08	−0.31
348.15	−45.45	−16.39	−22.04	1.00
358.15	−44.69	−15.30	−21.00	2.32
368.15	−43.93	−14.21	−19.96	3.63
378.15	−43.17	−13.12	−18.92	4.95
388.15	−42.42	−12.02	—	—
398.15	−41.66	−10.93	—	—
408.15	−40.90	−9.84	—	—
418.15	−40.14	−8.75	—	—
428.15	−39.39	−7.65	—	—
438.15	−38.63	−6.56	—	—
448.15	−37.87	−5.47	—	—
458.15	−37.12	−4.38	—	—
468.15	−36.36	−3.29	—	—
478.15	−35.60	−2.19	—	—
488.15	−34.84	−1.10	—	—
498.15	−34.09	−0.001	—	—
508.15	−33.33	1.08	—	—

Taking natural logarithms

$$\ln \frac{k}{T} = \ln\left(\frac{k_B}{T} e^{\Delta S^{\#}/R}\right) - \frac{\Delta H^{\#}}{RT}$$

The plot of ln k/T against $1/T$ gives a straight line with a slope $\Delta H^{\#}/R$ and intercept on the y-axis

$$\ln (k_B e^{\Delta S^{\#}/R})$$

from whence $\Delta H^{\#}$ and $\Delta S^{\#}$ can be determined.

Values of $\Delta H^{\#}$ and $\Delta S^{\#}$ for the systems with and without filler are given in Table VI. This table shows that $\Delta S^{\#}$ for both systems is less negative for the nth order path, while $\Delta H^{\#}$ is less negative for the autocatalytic one. This means that the nth order path for both systems is dominant for the formation of the activated complex. This behavior is in good agreement with that obtained by some authors.[5,14] On the other hand, comparison of data shows that for both mechanisms, nth order and autocatalyzed, $\Delta H^{\#}$ is less negative for the system without filler, while $\Delta S^{\#}$ is less negative for the system with filler. The same happens for the autocatalyzed path. This means that, for the filled system, both mechanisms coexist in a wide range of temperatures.

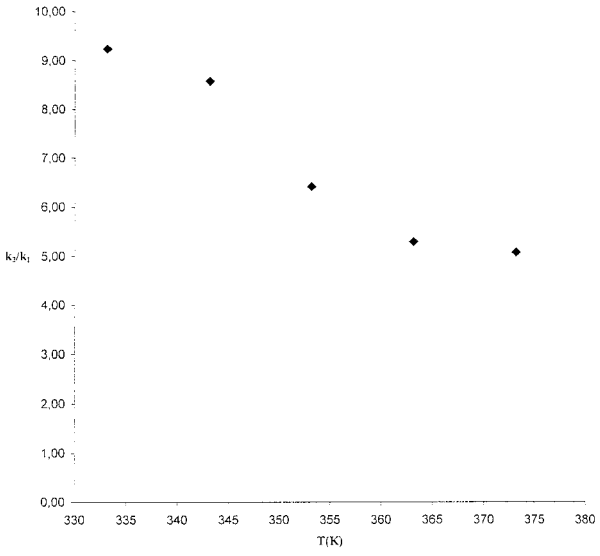

Figure 7 Plot of rate constants ratio, k_2/k_1, versus temperature.

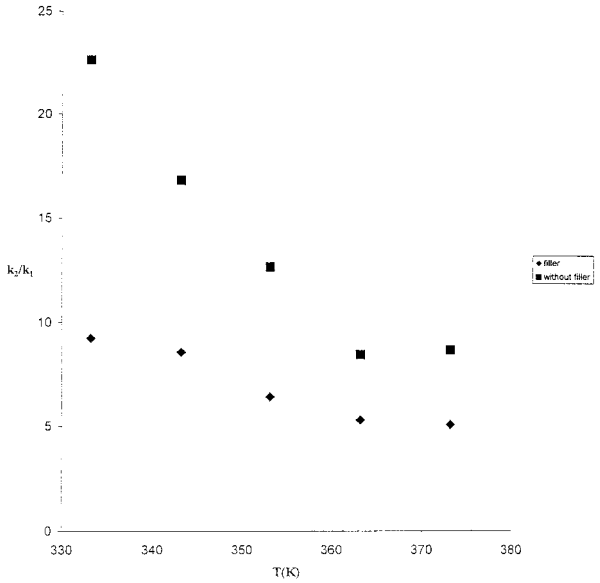

Figure 8 Plots of rate constants ratio, k_2/k_1, versus temperature for the system with and without filler.

Table VII gives values of $\Delta G_{n\text{-path}}$ and ΔG_{auto} at various temperatures for both systems. As can be seen, for the system without the filler, the nth order mechanism is predominant above 348 K, while for the system with the filler it is predominant above 508 K. As a consequence, for the filled system, the autocatalyzed mechanism is present in a wider range of temperatures, practically in the whole range of conversion.

Plot of k_2/k_1 rate versus T (Fig. 7) suggested a trend to the nth path mechanism with increasing temperatures. Figure 8 shows plots of k_2/k_1 rate versus T for the system with and without the filler. In this figure, it can be seen that at low temperatures the trend to the nth path mechanism is more favorable for the system without the filler.

REFERENCES

1. Horie, K.; Hiura, H.; Sawada, M.; Mita, I.; Kambe, H. J Polym Sci 1970, 8, 1357.
2. Kamal, M. R. Polym Eng Sci 1974, 14, 23.
3. Lee, H.; Neville, K. Handbook of Epoxy Resins; McGraw-Hill: New York, 1967.
4. May, C. A. Epoxy Resins: Chemistry and Technology; Marcel Dekker: New York, 1988.
5. Núñez, L.; Fraga, F.; Fraga, L.; Castro, A. J Polym Sci 1997, 63, 635.

6. Núñez, L.; Taboada, J.; Fraga, F.; Núñez, M. R. J Appl Polym Sci 1997, 66, 1377.
7. Núñez, L.; Fraga, F.; Núñez, M. R.; Villanueva, M. J Appl Polym Sci 1998, 70, 1931.
8. Barral, L.; Cano, J.; López, A. J.; López, J.; Nogueira, P.; Ramírez, C. J Appl Polym Sci 1995, 56, 1029.
9. Barton, J. M. Adv Polym Sci 1985, 72, 111.
10. Riccardi, C. C.; Adabbo, H. E.; Williams, R. J. J. J Appl Polym Sci 1984, 29, 2480.
11. Wasserman, S.; Johari, G. P. J Appl Polym Sci 1994, 53, 331.
12. Eyring, H. J Chem Phys 1935, 3, 107.
13. Evans, G.; Polyani, M. Trans Faraday Soc 1935, 31, 875.
14. Pazos Pellín, M.; Núñez, L.; López Quintela, A.; Paseiro, P.; Simal, J.; Paz, S. J Appl Polym Sci 1995, 55, 1507.